Global Journal of Researches in Engineering: C
Chemical Engineering
Volume 23 Issue 1 Version 1.0 Year 2023
Type: Double Blind Peer Reviewed International Research Journal
Publisher: Global Journals
Online ISSN: 2249-4596 & Print ISSN: 0975-5861

Modeling of CO Oxidation by Diffusion of Oxygen Atoms in Ceria-Zirconia Particulates in a Three-Way Catalyst Particle Membrane Filter

By Phyozin Koko & Katsunori Hanamura

Abstract- In order to design a microporous membrane filter comprising Three-way Catalyst (TWC) particles with a size distribution of 1 to 2 microns, isothermal CO oxidation experiments and numerical simulations were conducted to investigate the transport of oxygen atoms within primary Ceria-Zirconia (CZ) particulates. These spherical TWC particles were fabricated through the agglomeration of primary CZ and alumina particulates, incorporating Pd and Rh catalysts. By comparing experimental CO_2 emissions with simulation results over time, a temperature-dependent diffusion coefficient was determined. The simulation results reveal that the effective distance of oxygen atom transport within CZ particulates, heterogeneously distributed in the spherical TWC particle, is limited to approximately 100 nm from the surface of agglomerated spherical TWC particles within a temperature range of 175 to 225°C.

Keywords: *modeling, diffusion, three-way-catalyst, membrane particulate filter.*

GJRE-C Classification: *LCC Code: TJ807-83*

Strictly as per the compliance and regulations of:

Modeling of CO Oxidation by Diffusion of Oxygen Atoms in Ceria-Zirconia Particulates in a Three-Way Catalyst Particle Membrane Filter

Phyozin Koko [α] & Katsunori Hanamura [σ]

Abstract- **In order to design a microporous membrane filter comprising Three-way Catalyst (TWC) particles with a size distribution of 1 to 2 microns, isothermal CO oxidation experiments and numerical simulations were conducted to investigate the transport of oxygen atoms within primary Ceria-Zirconia (CZ) particulates. These spherical TWC particles were fabricated through the agglomeration of primary CZ and alumina particulates, incorporating Pd and Rh catalysts. By comparing experimental CO_2 emissions with simulation results over time, a temperature-dependent diffusion coefficient was determined. The simulation results reveal that the effective distance of oxygen atom transport within CZ particulates, heterogeneously distributed in the spherical TWC particle, is limited to approximately 100 nm from the surface of agglomerated spherical TWC particles within a temperature range of 175 to 225°C.**

Keywords: modeling, diffusion, three-way-catalyst, membrane particulate filter.

I. Introduction

It is essential to implement an efficient after treatment system for internal combustion engines during the transitional period until the full adoption of cleaner technologies is accomplished. To attain net-zero emission by 2050, exhaust gases from automobile engines have emerged as a significant contributor to air pollution, which is 25% of total CO_2 emission, currently ranked as a second largest source, leading to a global concern for their adverse effects on public health [1-3]. Therefore, an efficient and effective exhaust gas aftertreatment system plays an important role to reduce the solid and gaseous pollutant emissions from internal combustion engines. In conventional exhaust gas aftertreatment systems of gasoline-fueled engines, a gasoline particulate filter (GPF) is installed for filtration of solid particulate matters. Besides, a three-way catalytic converter (TWC) is used to simultaneously reduce harmful gaseous pollutants such as carbon monoxide (CO), nitrogen oxides (NO_x), and hydrocarbons (HCs) [4]. The literature has extensively been reported on the purification performance of combined TWC and GPF using wash-coating technology, commonly known as a catalyzed gasoline particulate filter (cGPF). Through application of catalyst materials deposited on the cGPF filter substrate, an integrated catalytic filter can offer a distinct advantage of not only trapping soot, but also facilitating the purification of gaseous pollutants in a single unit [5, 6]. However, the pressure-drop between the inlet and outlet of the integrated filter increases drastically because some pores are blocked by the coated TWC-paste.

Cerium oxides are well-established oxygen storage materials that have been widely used in various catalytic applications. They are particularly important as a catalytic component in TWCs installed in the exhaust gas aftertreatment systems of gasoline engines [7, 8]. The primary function of a TWC that includes cerium oxides is to simultaneously reduce three major gaseous pollutants, NO_x, CO, and HCs, through oxidation and reduction reactions. Maximal conversion yields can be achieved with an air-fuel ratio around the stoichiometric point for gasoline engines. If there are fluctuations in the oxygen concentration in the positive (fuel-lean) or negative (fuel-rich) direction around the stoichiometric point, excess oxygen can be stored by cerium oxides under a fuel-lean condition, while additional oxygen atoms can be supplied by cerium oxides under the fuel-rich conditions. The range of the air-fuel ratio for simultaneous reduction becomes slightly wider around the stoichiometric point as a well-known window [9, 10]. Ceria-zirconia (CZ) catalysts are commonly utilized to increase the oxygen storage capacity thereby enhancing the high-redox catalytic performance of ceria in TWCs. Since the exhaust gas temperature in gasoline-fueled engines typically reaches approximately 900°C, CZ is composited with alumina (Al_2O_3) to prevent the sintering effect or thermal degradation [11].

Recently, particle membrane filters have been manufactured by the authors using various catalyst components with the aim of improving soot oxidation kinetics and mitigating exhaust gas pollutants [12–14]. In contrast to wash-coated catalyzed particulate filters as mentioned above, catalyst particles were percolated as a membrane on the surface of a GPF substrate, which results in almost 100% filtration efficiency from the beginning of soot trapping and a low pressure-drop filter compared with the conventional filters [15]. By fabricating a particle membrane filter composed of three-way catalyst particles, in addition to a 100% initial

Author α σ: Department of Mechanical Engineering, School of Engineering, Tokyo Institute of Technology, Japan.
e-mail: koko.p.aa@m.titech.ac.jp

soot filtration efficiency, a simultaneous reduction of gaseous pollutants were achieved in a single unit [16]. Based on the findings from our previous parametric study on the fabrication of TWC particles membrane filters, the porosity of the TWC particle membrane reaches 64% under the condition of a mean particle size of 1.2 um and a superficial velocity of 5 mm/s [17]. The high porosity membrane filter contributes to low pressure-drop filtration of soot.

For the conventional TWC wash-coated filters [18, 19] and the conventional catalytic converters [20, 21], the macroscopic reaction kinetics modelling has been extensively developed and the microscopic transport of oxygen atoms in ceria has been reported [22 – 25] under the condition of the practical temperature above 700°C. However, if the thermal efficiency of engines for passenger's vehicles can be increased up to more than 50% (already reached up to 52.63%) to reduce emission of CO_2, the exhaust gas temperature at the engine out will be decreased around 300°C to 400°C [26]. By utilizing the TWC particles membrane filter proposed by the authors, it is feasible to achieve not only almost 100% initial soot filtration efficiency with low pressure-drop but also simultaneous reduction of exhaust gas pollutants as an integrated after-treatment system even under such a low temperature condition. For effective utilization of CZ particulates for chemical reaction, the transport phenomena of oxygen atom around the single primary CZ particulate should be investigated. Using the spherical agglomerated TWC particle including primary CZ particulates manufactured by the authors, the oxygen atom transport in the CZ can be analyzed by a simplified mathematical model compared with the conventional TWC wash-coated filters. In the current study, the diffusion coefficient of the oxygen atom in CZ particulate is determined through experiment and numerical simulation. Besides, the transport distance of oxygen atom in the CZ for CO oxidation is clarified under the condition of a range of temperature from 175°C to 225°C.

II. Experimental Procedures

Figure 1 describes a miniature-sized particulate filter with a precise dimension as length x width x height (10 mm x 10 mm x 10 mm), comprised of 7x7 square channels. The miniature-sized filter substrate sample was extracted from conventional silicon carbide (Si-C) substrates of full-sized particulate filters. A high-temperature-resistant ceramic paste was utilized to seal alternating ends of the channels to create a wall-flow configuration, as illustrated in Fig. 2, in which the working gas passes through the channel walls.

Figure 3 displays a schematic diagram of the fabrication process of a three-way catalyst (TWC) particle membrane filter on a miniature filter

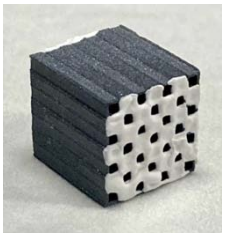

Fig. 1: Miniature particulate filter made of Si-C

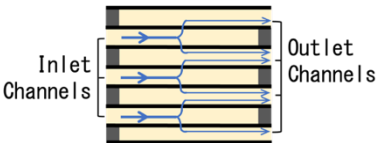

Fig. 2: Schematic of a wall-flow filter

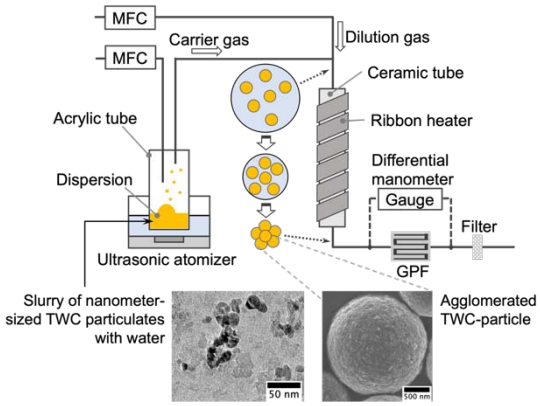

Fig. 3: Schematic diagram of the manufacturing process of TWC-particle membrane filter

Table 1: Chemical composition of TWC slurry

Chemical compounds		Composition (%)
Palladium oxide	PdO	1.45
Rhodium oxide	Rh_2O_3	0.26
Cerium dioxide	CeO_2	18.3
Zirconium dioxide	ZrO_2	26.10
Aluminum oxide	Al_2O_3	47.70
Lanthanum oxide	La_2O_3	3.28
Neodymium oxide	Nd_2O_3	2.90

substrate. The experimental procedure and fabrication process were discussed in detail in the previous literature [17]. The slurry used in its fabrication was comprised of 20 wt.% of primary nanometer-sized TWC particulates prepared using distilled water. These particles had an average diameter of approximately 200 nm, as shown in the TEM image in Fig. 3. The chemical composition of the primary TWC-particulates is the same as that of a commercial monolith converter, as shown in Table 1. The TWC particulate slurry was introduced into an acrylic tube to generate small droplets with a size range of 5-10 um using an ultrasonic atomizer (60 Hz frequency). Nitrogen gas was

introduced into the acrylic tube at a flow rate of 50 mL/min to transport the atomized water droplets, including TWC particulates from the tube. The gas-suspended droplets containing TWC particulates were then mixed with a dilution gas to achieve a superficial velocity of 5 mm/s and a humidity lower than the dew point, even at room temperature. Nitrogen gas-diluted dispersed water droplets were introduced into an evaporator, which was kept at constant temperature of 280°C using a ribbon heater. Since only water was vaporized, the primary TWC particulates agglomerated, as shown in the SEM image of Fig. 3. The agglomerated nitrogen dispersed TWC particles, ranging in size from 1 to 2 μm, were deposited as a membrane layer onto a miniaturized filter substrate. Then, as in our previous study, the fabricated membrane filter was sintered at 900°C for 4 hours to maintain the percolation structure of the TWC membrane with a minimal peeling rate [27].

A scanning electron microscopic (SEM) cross-sectional image of a TWC particle membrane filter on a substrate is presented in Fig. 4. The thickness of the membrane layer is approximately 40 microns in which the agglomerated TWC particles (arithmetic mean diameter of 1.2 um) are percolated. The porosity of the membrane was measured as approximately 64.4% [17]. The size of the agglomerated TWC particles was controlled by adjusting the weight percentage of the primary TWC particulates in the slurry. The primary TWC particulates are homogeneously dispersed throughout the entire cross-sectional area of a single agglomerated TWC particle, as shown in the SEM images of Fig. 4.

However, using a back-scattered electron mode, a non-homogeneous composition distribution was observed, as shown in Fig. 5(a). In this figure, the bright colored areas are ceria-zirconia (CZ) particulates since CZ has the highest atomic number compared to the other components of the slurry. The dark gray areas were identified as aluminum oxide particulates. The ratio of these areas was analyzed using Image-J program. The results presented in Fig. 5(b) revealed that the average CZ-particulate area occupied approximately 50% of the whole cross-sectional area of a single agglomerated TWC particle.

Figure 6 shows a schematic diagram of an isothermal CO oxidation experimental setup. A working gas consisting of CO (44 ppm) with the balance as N_2, was introduced (with no oxygen supplied in the working gas) through the TWC particle membrane at a superficial velocity of 20 mm/s and temperatures of 175, 200 and 225°C to investigate the transport of oxygen atoms in the TWC particles. Temperature was measured using a thermocouple inserted in an outflow channel of the substrate filter. It was fixed by an electric heater with a PID feedback system. The concentrations of CO and CO_2 were measured as a function of time using an infrared gas analyzer after the gas stream was passed through the membrane. The supplied CO concentration was calibrated after each measurement under each temperature condition using a by-pass line. Before the experiment, all pre-adsorbed gas molecules on the catalyst surface were removed by passing N_2 gas through the membrane.

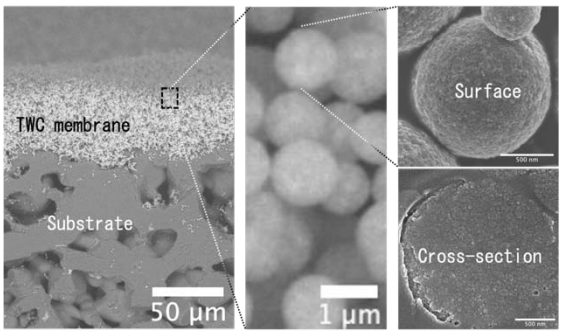

Fig. 4: Surface and cross-sectional morphology of agglomerated TWC-particles

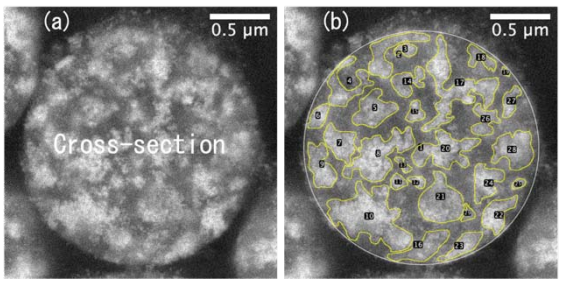

Fig. 5: Elemental analysis of the cross-section of an agglomerated TWC-particle using a back-scattered electron mode

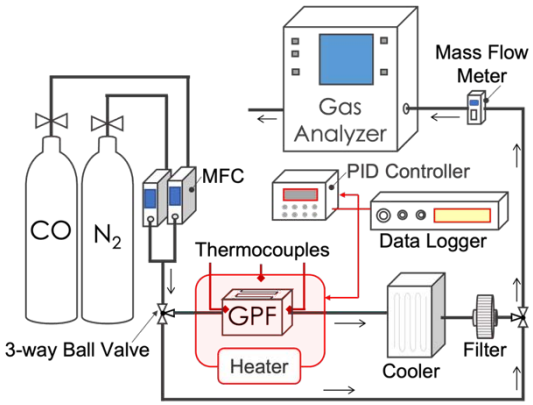

Fig. 6: Experimental setup of CO oxidation measurement through a TWC-particle membrane

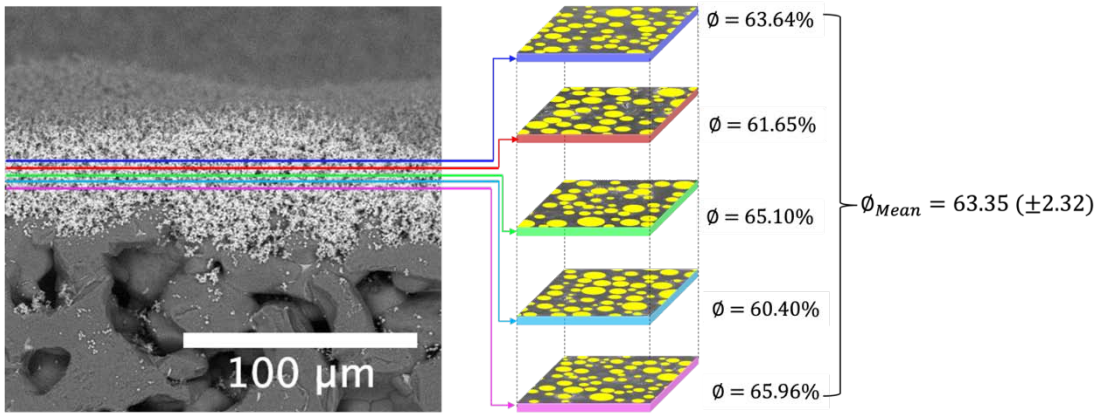

Fig. 7: Measurement of Porosity (ϕ) distribution through image processing analysis showing a homogeneous porous medium along the membrane thickness

III. Numerical Simulation

In the numerical simulation model, the following assumptions were made:

1) The agglomerated particle sizes were assumed to be as the same as the arithmetic mean diameter, 1.2 um.
2) Diffusion of oxygen atoms from CZ-particulates was assumed to be an isotropic process, involving one-dimensional diffusion from the bulk of a particulate to the surface (in the x-direction).
3) The chemical reaction occurred at the surface of spherical agglomerated particles by reacting with diffused oxygen atoms from the bulk of CZ-particulates.
4) The temperature of working gas along the membrane thickness direction (z-direction as depicted in the Fig. 8) was uniform during the reaction. Because the generated heat by the exothermic reaction is negligibly small which cannot vary the working gas temperature.
5) The oxygen concentration of TWC-particles percolated in the same location in the discrete volume of the membrane with a uniform concentration throughout the reaction.

As described in Fig. 7, the porosity (ϕ) distribution was consistent (with a discrepancy of ±2.32%) along the membrane thickness direction (z-direction) since the percolation structure of the spherical TWC-particles membrane consists of a homogeneous porous medium [17]. In such a medium, the properties of a percolation structure, such as porosity and permeability, are constant throughout the medium. This uniformity means that the flow characteristics and the resistance to flow are the much the same in all directions. Besides, the tortuosity of the membrane was estimated as small as 1.02013. Therefore, a straight flow characteristic along the membrane thickness direction was assumed in this model. Additionally, from an order estimation of the convective, pressure drop and viscous

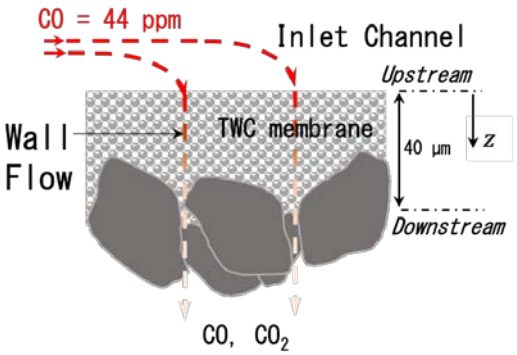

Fig. 8: Schematic of the CO concentration distribution in a three-way catalyst membrane

terms of the Navier Stokes equations under the experimental conditions, the pressure drop and viscous terms are dominant. In fact, the Reynolds number along the membrane is as low as 0.027. Therefore, the working gas flow in this direction becomes the lowest pressure drop, *i.e.*, flow in the z-direction is perpendicular to the membrane layer. As a result, even if the working gas is introduced in the channel direction, from left to right in Fig. 8, the average velocity in the membrane can be assumed to be unidirectional and in the *z*-direction.

Figure 8 shows a schematic diagram of streamlines in the membrane filter. Here, the working gas is fed into the membrane layer through an inlet channel in a wall-flow pattern in a uniformly distributed manner. Assuming a one-dimensional, incompressible and uniform flow with a characteristic velocity (superficial velocity) at the membrane layer, only a decrease in CO concentration through oxidation should be considered along the flow direction (in the z-direction). Additionally, it was hypothesized that CO reacts with oxygen atoms diffused from the inside of the CZ material, and the reaction occurs at the TWC particle surfaces as follows.

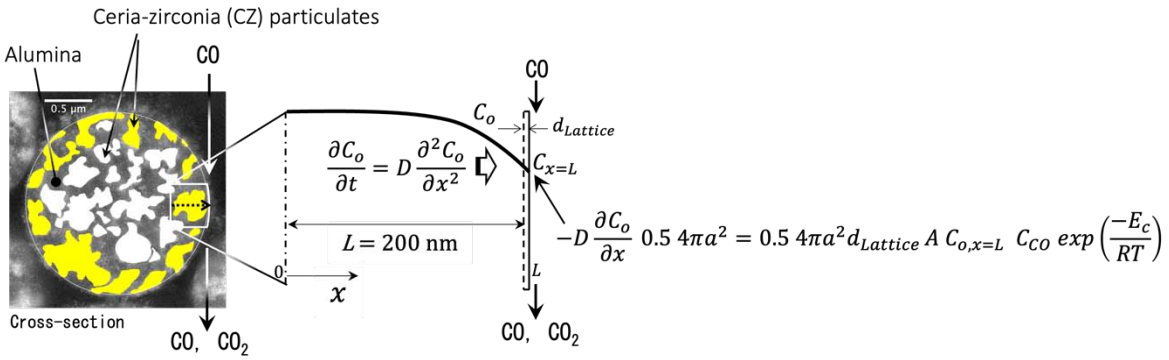

Fig. 9: Schematic image of diffusion-controlled CO oxidation in a three-way catalyst particle membrane model

$$CO + O_{diff} \rightarrow CO_2 \quad (1)$$

$$\frac{\partial C_{CO}}{\partial t} + u\frac{\partial C_{CO}}{\partial z} = 0.5\ n\ 4\pi a^2 d_{Lattice}\ \ C_{O,x=L}\ A\ C_{CO}\ exp\left(\frac{-E_c}{RT}\right) \quad (2)$$

The rate of the reaction can be expressed as an Arrhenius-type equation that is proportional to the CO concentration, the number of oxygen atoms present at the TWC particle surface, and the number density of TWC particles. Thus, the governing equation can be written as Eq. 2.

Here, the concentration of CO (C_{co}), superficial velocity (u), time (t), space axis in the flow direction (z), number of TWC particles in a unit volume (*n*), radius of the TWC particle (*a*), lattice constant of CZ material ($d_{Lattice}$), oxygen atom concentration in the CZ material ($C_{o,x=L}$), activation energy for oxidation at the surface of a TWC particle (E_c), gas constant (*R*), and absolute temperature (*T*) are all parameters in the governing equation (Eq. 2). This equation describes the reaction rate as an Arrhenius-type expression that is proportional to the CO concentration, the number of oxygen atoms at the TWC particle surface, and the number density of TWC particles. The product of $4\pi a^2$ and $d_{lattice}$ represents a thin shell volume at the TWC particle surfaces. The lattice constant of CZ material ($d_{lattice}$) was 0.5 nm, obtained from previous work [28]. The factor, 0.5, on the right-hand side of Eq. (2) represents the CZ surface area ratio, 50%, in the spherical surface area of the TWC particles, which is discussed below. Transport of oxygen atoms by diffusion in the CZ material should be simultaneously calculated to obtain the oxygen atom concentration at the TWC particle surfaces.

In the simulation, a volume averaging method was used along the membrane thickness (z-direction). The oxygen concentration of the particles varies with respect to their location in the membrane. Therefore, a discrete thickness of 4 um was considered as a control volume that contained approximately 1.28 x 10^9 particles. The total number of particles percolated in a control volume with a particular thickness can be calculated using Eq. 3.

$$S\ L\ \varepsilon = N\ \frac{4}{3}\ \pi\ r^3 \quad (3)$$

where *S* is the total surface area of the membrane, *L* is the thickness of the membrane, ε is the packing fraction of the membrane, *N* is the total number of particles and *r* is the particle radius.

In Fig. 9, a schematic illustration of diffusion-controlled CO oxidation is presented. The initial oxygen concentration volume was calculated according to the oxygen vacancy concentration (66.67%) and the lattice parameter (0.5 nm) of the ceria-zirconia material [11, 28]. According to back-scattered electron imagery using FESEM, the primary CZ-particulates were heterogeneously distributed in a spherical agglomerated particle as mentioned in Fig. 5. Individual CZ-particulates were separate from each other. CZ-particulates located at the surface of the single spherical agglomerated particle (yellow-colored CZ-particulates in Fig. 5) contribute to oxygen atom supply. Here, CO molecules flowing along the spherical surface react with the supplied oxygen atoms at the interfaces between the gas phase and the exposed CZ-particulate surfaces. Therefore, it can be assumed that the oxygen atoms will be transported to the surface (to the interface) from the inside of the bulk material, one-dimensionally in the *x*-direction, as shown in Fig. 9. Therefore, a one-dimensional diffusion equation for oxygen atoms in the *x*-direction can be expressed as Eq. 4.

$$\frac{\partial C_o}{\partial t} = D\frac{\partial^2 C_o}{\partial x^2} \quad (4)$$

Here, C_o represents oxygen atom concentration, *t* is time, *x* is the axis from the inside to the surface of the CZ and *D* is the diffusion coefficient of oxygen atoms in the CZ material.

$$D = D_0\ exp\left(\frac{-E_a}{RT}\right) \quad (5)$$

According to the experimental results of isothermal CO conversion, emissions of CO_2 were increased at higher temperatures, as shown in Fig. 10.

The experimental results show that the logarithmic function of the diffusion rate was proportional to the inverse of absolute temperature. From this linearity, the Arrhenius-type expression is suitable for representing the diffusion of oxygen atoms over the temperature range of the current study. The diffusion coefficient is an Arrhenius type expression described in Eq. 5, where D_o is the pre-exponential diffusivity and E_a is the activation energy for diffusion.

The boundary conditions for $x = 0$ and $x = L$ are expressed as Eq. 6 and 7, respectively. There is no diffusion at $x = 0$, while the molar flux of oxygen atoms obtained from the concentration gradient at $x = L$ in the CZ material is equal to the consumption rate of CO by oxidation at the TWC particle surfaces as follows.

$$\frac{\partial C_O}{\partial x} = 0 \qquad at\ x = 0 \tag{6}$$

$$-D\frac{\partial C_O}{\partial x} = A\, d_{Lattice}\quad C_{O,x=L}\quad C_{CO}\, exp\left(\frac{-E_c}{RT}\right)\quad at\ x = L \tag{7}$$

The process of fitting oxygen atom flux data, obtained from both experimental and numerical simulations, was initiated at a temperature of 175°C. Since the diffusion coefficient governing the transport of oxygen atoms within the CZ particulate is an unknown value, an inverse approach was employed to estimate the diffusion coefficient, denoted as D in Eq. 4. Additionally, for CO oxidation at the agglomerated TWC particle surfaces, the pre-exponential factor A needed to be estimated by fitting the time history of the oxygen atom flux. This approach involved iteratively adjusting both the diffusion coefficient D and collision frequency A values while fitting the time history of the oxygen atom flux at the TWC particle surface. In accordance with Eq. 7, altering the D values results in a change in the slope of the curve, whereas adjustments to the A values lead to variations in the flux amount (i.e., along the y-axis in Figure 11). Once a good agreement between experimental and numerical results was achieved at 175°C, higher D values were used for the higher temperature conditions (i.e., 200°C and 225°C) while maintaining the same A values. The activation energy E_a and pre-exponential diffusivity D_o in Eq. 5 were simultaneously estimated from an Arrhenius plot. Here, a straight-line relationship in the plot was iterated multiple times by changing various D values, until the goodness of fit was achieved up to 0.998. The activation energy E_c was 9 kJ/mol, obtained from earlier literature [29, 30]. The mean radius of the TWC particle a and the mean size of the primary CZ particulate L are assumed to be 0.6 nm and 200 nm, respectively, based on SEM and TEM images obtained in the experiment.

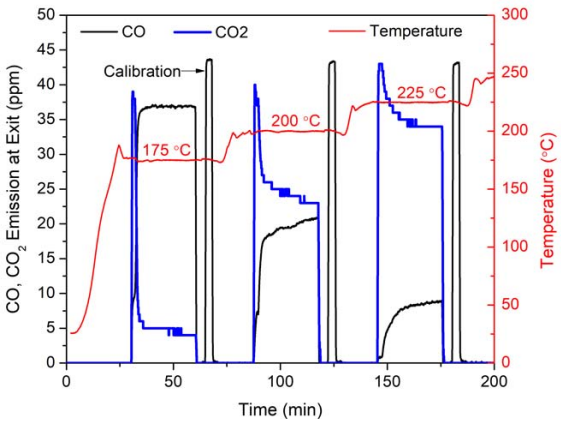

Fig. 10: Isothermal CO oxidation by a TWC membrane at 175, 200 and 225°C

Table 2: Summary of fitted diffusion parameters

Temperature (°C)	Diffusion coefficient, D (m^2 sec^{-1})	Collision Frequency, A (m^3 mol^{-1} sec^{-1})
175	2.3×10^{-19}	1.55×10^{9}
200	8.4×10^{-19}	
225	3.1×10^{-18}	

IV. Results and Discussion

Figure 10 presents the experimental results of isothermal CO oxidation by TWC particle membranes at different temperatures (175, 200, and 225°C). The temperature of the miniature-sized filter with the membrane is indicated in red color on the right-hand side vertical axis. It is increased using an electric heater under a nitrogen atmosphere. At the start of the experiment, CO (44 ppm) was introduced with the temperature fixed at 175°C. The black and blue lines illustrate emissions of CO and CO_2, respectively. After 30 minutes, CO and CO_2 emissions were approximately 7% and 37%, respectively. Therefore, a significant amount of CO was oxidized by the TWC particle membrane, even in the absence of supplied oxygen. However, CO_2 emissions decreased over time while CO emissions increased. The isothermal CO oxidation experiment was stopped after 30 minutes. Before proceeding with the next higher temperature experiment, the supplied CO concentration was confirmed as 44 ppm. This cycle represents an isothermal CO oxidation experiment for one temperature condition. With increased temperature, from 175 to 225°C, the initial CO emission approaches to zero, and the decrease in CO_2 emission was not significant. Furthermore, it was observed that CO_2 emission does not decrease over time when the temperature exceeds 300°C.

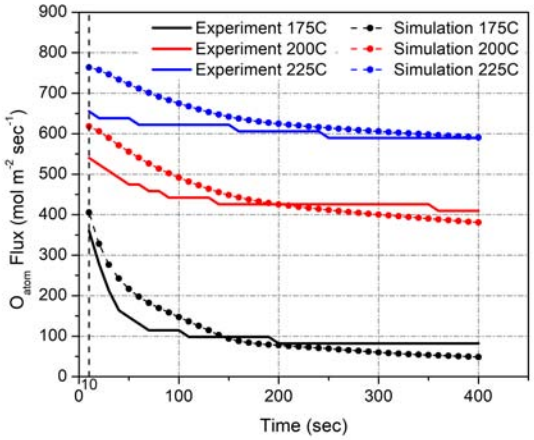

Fig. 11: Fitting of oxygen atom flux

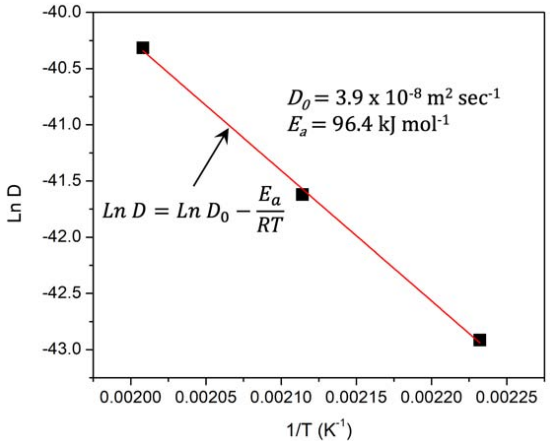

Fig. 12: Arrhenius plot for activation energy and pre-exponential factor of oxygen atom diffusion

Figure 11 shows fitting results between experimental and numerical oxygen atom fluxes at the TWC particle surfaces. Here, the oxygen atom flux in the experiment was estimated from the required number of oxygen atoms to produce one mole of CO_2, calculated from emission concentrations with respect to time. In numerical simulation, the flux was obtained from the gradient of oxygen atom concentration at the surface of the CZ material. The fitting parameter *A*, which is the pre-exponential factor for oxidation, contributes to an increase or a decrease in flux in the entire region during the elapsed time. *D* is the diffusion coefficient of oxygen atoms that contributes to a decreasing rate of flux over time. The numerical results agree well with the experimental data using a combination of fitting parameters, shown in Table 2. There were some discrepancies in the data at the beginning of oxidation, especially at higher temperatures. The concentration of introduced CO was initially stepwise in the numerical simulation, while there was a gradually increased initial condition, from 0 to 44 ppm, in the experiment. Therefore, to remove uncertainties at the initial times, the calculated oxygen atom flux from the experiment was fitted starting from 10 seconds until the end of measurement (i.e., 400 seconds), as shown in Fig. 10. Using the obtained diffusion coefficient D from the fitting, the activation energy Ea and pre-exponential factor Do were estimated as 96.4 kJ/mol and 3.904 x 10-8 m2/s from the Arrhenius plot, as shown in Fig. 12.

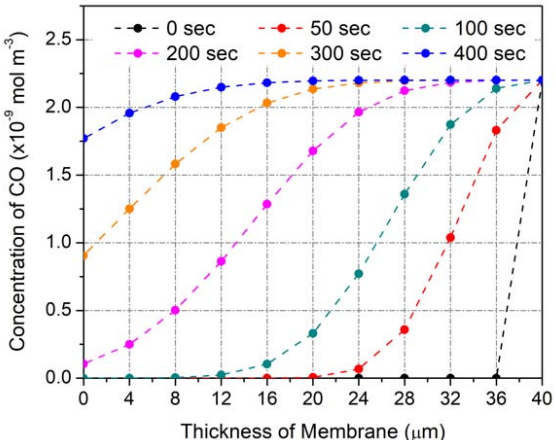

(a) 175°C

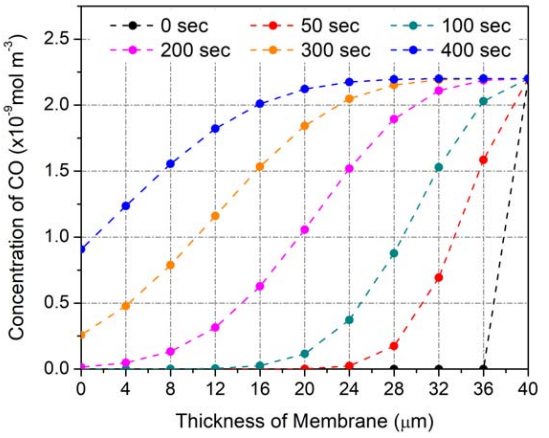

(b) 200°C

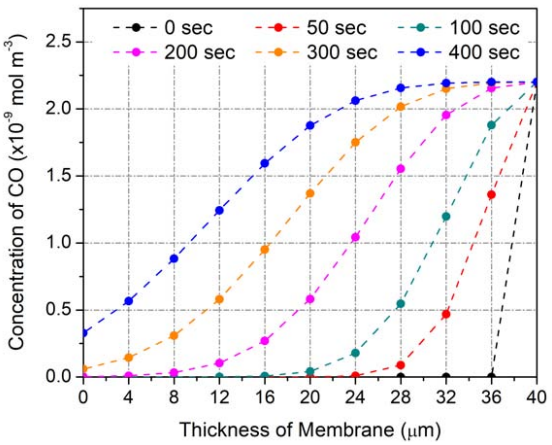

(c) 225°C

Fig. 13: Concentration distribution of CO along the membrane thickness at 175°C (a), 200°C (b) and 225°C (c)

Figure 13 shows variation of CO concentration distributions along the flow direction with respect to time from the beginning to an elapsed time of 400 seconds at 175, 200 and 225°C using the fitting parameters obtained above. Here, the working gas flows from the right to the left with a superficial velocity of 20 mm/s, and the concentration of CO at the right-hand side is fixed at 2.2 x 10^{-9} mol/m^3 (44 ppm). The concentration of introduced CO was decreased along the thickness by CO oxidation in the membrane, even at 175°C (Fig. 13(a)). There was no emission of CO for up to 100 seconds, although this doesn't agree with the experimental results. However, the CO concentration in entire region of the membrane was increased with respect to time due to a decreased oxidation rate even under an isothermal oxidation condition. Then, 400 seconds later, a high level of CO was emitted in the case of 175°C (Fig. 13(a)). With increased temperature, from 175 to 225°C, the emission at 400 seconds was less since more CO was oxidized.

Figures 14(a), 14(b) and 14(c) show variations of oxygen atom concentration distributions in the CZ material in a TWC particle located at the top surface of the membrane with respect to time at 175, 200 and 225°C, respectively. However, Figs. 15 and 16 show the same data at the middle and bottom surfaces of the membrane. The concentration gradient at the bottom surface of the membrane is smaller than that of the top and middle since the CO concentration decreases along the flow direction. Here, since at the right-hand end of each graph, oxygen reacts with CO and the oxygen concentration was decreased with respect to time. According to the CO oxidation rate at the right-hand end, oxygen is supplied by diffusion from the inside of the CZ particulate. As a result, the oxygen concentration was decreased in the *x*-direction at each time step. Moreover, with consumption of oxygen atoms, its concentration in the CZ particulate was decreased with time. With increasing temperature, from 175 (Fig. 14(a)) to 225°C (Fig. 14(c)), since the diffusion coefficient of oxygen atoms is increased as predicted by the Arrhenius expression, the concentration gradient at the surface (at the right-hand end) becomes smaller while the transport range becomes wider.

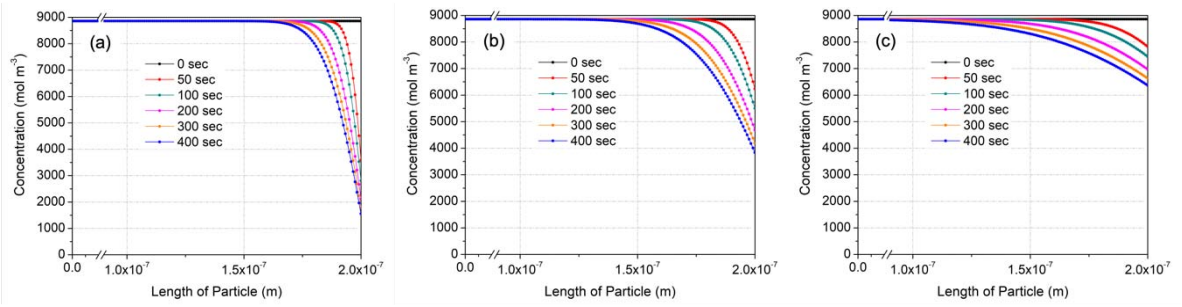

Fig. 14: Concentration profiles of CZ-particulates located at the upstream side of the membrane at 175°C (a), 200°C (b) and 225°C (c)

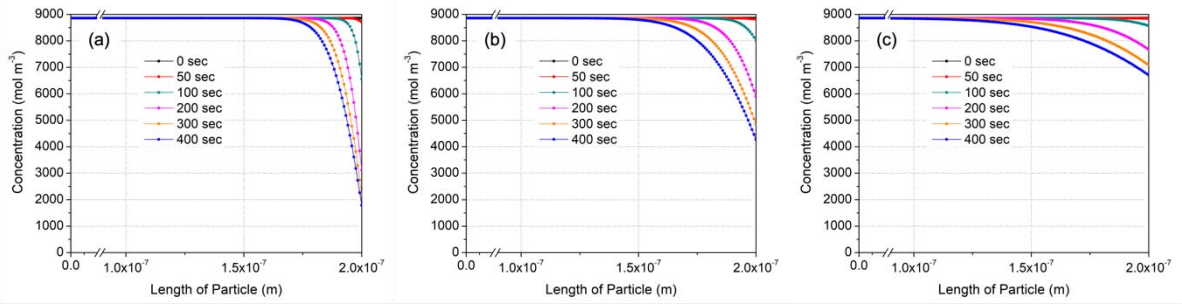

Fig. 15: Concentration profiles of CZ-particulates located at the middle of the membrane at 175°C (a), 200°C (b) and 225°C (c)

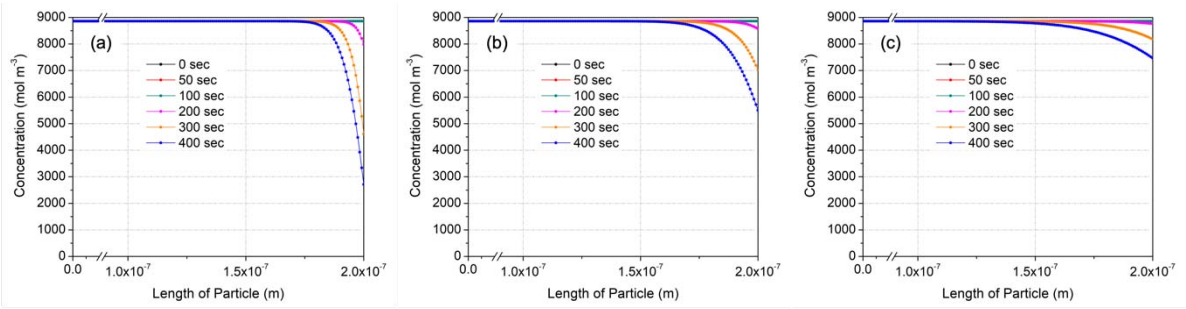

Fig. 14: Concentration profiles of CZ-particulates located at the downstream side of the membrane at 175°C (a), 200°C (b) and 225°C (c)

V. Conclusions

In this study, the diffusion-controlled oxygen transport process in ceria-zirconia (CZ) particulates located at the surface of the spherical TWC particles, which are the elements of the TWC particle membrane filter, was investigated through isothermal CO oxidation experiments and numerical modeling. Although the electron micrograph of cross-sectional view of a spherical TWC particle was exhibited as a homogeneously agglomerated structure, the primary CZ particulates were separated from each other within alumina at the spherical surface under a back-scattered electron mode. Moreover, the simulation results revealed that the oxygen atoms transport range of approximately 100 nm from the surface of the CZ particulates were mainly contributed to the reaction under a low temperature range of 175°C to 225°C. A few microns-sized TWC particles membrane wall-flow filter will become useful for a low-temperature exhaust gas due to the high specific surface area to enhance the purification reaction though the oxygen atom transport range is limited as obtained here.

Acknowledgement

This paper is obtained as a result of a grant project (JPNP21014) conducted by The Research Association of Automotive Internal Combustion Engines (AICE) with support from the New Energy and Industrial Technology Development Organization (NEDO). The author(s) would like to express their sincere gratitude to them.

References Références Referencias

1. Khalifa AA, Ibrahim AJ, Amhamed AI, El-Naas MH(2022) Accelerating the transition to a circular economy for net-zero emissions by 2050: A systematic review. Sustainability 14(18):410-430 https://doi.org/10.3390/su141811656
2. Krause J, Thiel C, Tsokolis D (2020) EU road vehicle energy consumption and CO2 emissions by 2050 – Expert-based scenarios. Energy Policy 138:134-147 https://doi.org/10.1016/j.enpol.2019.111224
3. Twigg, MV (2011) Catalytic Control of Emissions from Cars. Catalysis Today 163:33-41 https://doi.org/10.1016/j.cattod.2010.12.044
4. Joshi A, Johnson TV (2018) Gasoline particulate filters – A review. Emission control science and technology 4:219-239 https://doi.org/10.1007/s40825-018-0101-y
5. Qian Y, Li Z, Yu, Wang X, Lu X (2019) Review of the state-of-the-art of particulate matter emissions from modern gasoline fueled engines. Applied Energy 238:1269-1298 https://doi.org/10.1016/j.apenergy.2019.01.179
6. Richter J M, Klingmann R, Spiess S, Wong K (2012) Application of catalyzed gasoline particulate filters to GDI vehicles. SAE International Journal of Engines 5(3):1361-1370 https://doi.org/10.4271/2012-01-1244
7. Montini T, Melchionna M, Monai M, Fornasiero P (2016) Fundamentals and catalytic applications of CeO_2-based materials. Chemical Reviews 116(10):5987-6041 https://doi.org/10.1021/acs.chemrev.5b00603
8. Melchionna M, Fornasiero P (2014) The role of ceria-based nanostructured materials in energy applications. Materials Today 17 (7):349-357 https://doi.org/10.1016/j.mattod.2014.05.005
9. Wang J, Chen H, Hu Z, Yao M, Li Y (2014) A review on the Pd-based three-way catalyst. Catalysis Reviews57(1):79-144 https://doi.org/10.1080/01614940.2014.977059
10. Li P, Chen X, Li Y, Schwank JW (2019) A review on oxygen storage capacity of CeO_2-based materials: Influence factors, measurement techniques, and applications in reactions related to catalytic automotive emission control. Catalysis Today 327:90-115 https://doi.org/10.1016/j.cattod.2018.05.059
11. Suzuki T, Morikawa A, Suda, A (2002) Alumina-Ceria-Zirconia composite oxide for three-way catalyst, Special Issue Oxygen Storage Materials for Automotive-Ceria-Zirconia Solid Solution, R&D Review of Toyota CRDL 37(4):28-33.
12. Suteerapongpun T, Kitagawa Y, Srilomsak M, Hanamura K (2020) Development of membrane filter

made of alumina and silver-palladium particles for high-filtration efficiency, low-pressure drop and low-soot oxidation temperature. International Journal of Automotive Engineering 11(4):51-158 https://doi.org/10.20485/jsaeijae.11.4_151
13. Hanamura K, Inaba M, Kawabe K, Mitarai K (2022) Oxidation enhancement of particulate matters deposited on catalyzed membrane filter by nitrogen oxides diffusion. Transactions of Society of Automotive Engineers of Japan 53(1):100-106 https://doi.org/10.11351/jsaeronbun.53.100
14. Karin P, Hanamura K (2010) Microscopic visualization of particulate matter trapping and oxidation behaviors in a diesel particulate catalyst-membrane filter. JSAE Annual Congress Research Paper 41(4):853-858 https://doi.org/10.11351/jsaeronbun.41.853
15. Nakajima S, Sanui R, Hanamura K (2017) Soot trapping by high-permeability porous membrane filter made of aggregates of alumina nanoparticles. International Journal of Automotive Engineering 8(3):105-111 https://doi.org/10.20485/jsaeijae.8.3_105
16. Hanamura K, Fujii S, Teerapat S (2023) A study of multi-functional membrane filters made of fine catalyst particles. SAE Technical Paper 2023-32-0125.
17. Koko P, Suteerapongpun T, Hanamura K (2023) Measurement of porosity in three-way catalyst particles membrane filter using electron microscopy image analysis. International Journal of Automotive Engineering 14(1):27-34 https://doi.org/10.20485/jsaeijae.14.1_27
18. Taibani AZ and Kalamkar V (2012) Experimental and computational analysis of behavior of three-way catalytic converter under axial and radial flow conditions. International Journal of Fluid Machinery and Systems 5(3):134:142 https://doi.org/10.5293/IJFMS.2012.5.3.134
19. Tsinglou DN, Koltsakis GC, Peyton Jones JC (2002) Oxygen storage modeling in three-way catalytic converters. Industrial and Engineering Chemistry Research 41(5):1152:1165 https://doi.org/10.1021/ie010576c
20. Yamauchi T, Kubo S, Mizukami T, Sato N, Aono N (2011) Numerical simulation for optimal design of a multifunctional three-way catalytic converter with detailed chemistry. R&D Review of Toyota CRDL 42(1):33:42.
21. Walter R, Neumann J, Hinrichsen O (2022) A model-based analysis of washcoat distribution on zoned coated gasoline particulate filters. Chemical Engineering Journal 441:135615 https://doi.org/10.1016/j.cej.2022.135615
22. Yashiro K, Onuma S, Kaimai A (2002) Mass transport properties of $Ce_{0.9}Gd_{0.1}O_{2-\delta}$ at the surface and in the bulk. Solid State Ions 152-153:469-476 https://doi.org/10.1016/S0167-2738(02)00375-2
23. Ackermann S, Scheffe JR, Steinfeld A (2014) Diffusion of oxygen in ceria at elevated temperatures and its application to H_2O/CO_2 splitting thermochemical redox cycles. The Journal of Physical Chemistry 118:5216-5225 https://doi.org/10.1021/jp500755t
24. Stan M, Zhu YT, Jiang H, Butt D (2004) Kinetics of oxygen removal from ceria. Journal of Applied Physics 95(7):3358-3361 https://doi.org/10.1063/1.1650890
25. Nagasawa T, Kobayashi A, Sato S, Kosaka H, Kim K, You HM, Hanamura K, Terada A, Mishima T (2023) Visualization of oxygen storage process in Pd/CeO_2-ZrO_2 three-way catalyst based on isotope quenching technique. Chemical Engineering Journal 453:139937 https://doi.org/10.1016/j.cej.2022.139937
26. Nagasawa T, Okura Y, Yamada R, Sato S, Kosaka H, Yokomori T, Lida N (2021) Thermal efficiency improvement of super-lean burn spark ignition engine by stratified water insulation on piston top surface. International Journal of Engine Research 22(5): 1421-1439 https://doi.org/10.1177/1468087420908164
27. Arai S, Fujii S. Koko P, Suteerapongpun T, Hanamura K (2023) Durability of three-way-catalyst-particles membrane filter for fluid-dynamic shear stress. International Journal of Automotive Engineering 54(3):141-152 https://doi.org/10.11351/jsaeronbun.54.566
28. Gul SR, Khan M, Zeng Y, Lin M, Wu B, Tsai C (2018) Electronic band structure variations in the ceria doped zirconia: A first principles study. Materials 11(7):329-341 https://doi.org/10.3390%2Fma11071238
29. Christou SY, Costa CN, Efstathiou, AM (2004) A two-step reaction mechanism of oxygen release from Pd/CeO2: Mathematical modelling based on step gas concentration experiments. Topics in Catalysis 30:325-331 https://doi.org/10.1023/B:TOCA.0000029770.40236.44
30. Christou SY, Costa CN, Efstathiou, AM (2003) Mathematical modeling of the oxygen storage capacity phenomenon studied by CO pulse transient experiments over Pd/CeO2 catalyst. Journal of Catalysis 219:259-272 https://doi.org/10.1016/S0021-9517(03)00151-9